Unconditionally stable second-order accurate scheme for a parabolic sine-Gordon equation

Seokjun Ham; Youngjin Hwang; Soobin Kwak; Junseok Kim ✉ iD

Check for updates

View Online

Export Citation

Articles You May Be Interested In

Well-posedness results for a generalized Klein-Gordon-Schrödinger system

J. Math. Phys. (October 2019)

Sasa-Satsuma (complex modified Korteweg–de Vries II) and the complex sine-Gordon II equation revisited: Recursion operators, nonlocal symmetries, and more

J. Math. Phys. (April 2007)

Numerical simulation of two dimensional sine-Gordon solitons using modified cubic B-spline differential quadrature method

AIP Advances (January 2015)

Unconditionally stable second-order accurate scheme for a parabolic sine-Gordon equation

View Online   Export Citation   CrossMark

Seokjun Ham, Youngjin Hwang, Soobin Kwak, and Junseok Kim[a] (iD)

AFFILIATIONS

Department of Mathematics, Korea University, Seoul 02841, Republic of Korea

[a]Author to whom correspondence should be addressed: cfdkim@korea.ac.kr. **URL:** https://mathematicians.korea.ac.kr/cfdkim/

ABSTRACT

In this study, we propose an unconditionally stable temporally second-order accurate scheme for a parabolic sine-Gordon equation. The proposed scheme is based on an operator splitting method. We solve linear and nonlinear equations using a Fourier spectral method and a closed-form solution, respectively. The proposed numerical method is temporally second-order accurate and unconditionally stable. To verify the superior efficiency and accuracy of the proposed scheme, we conduct various numerical tests. Computational tests validate the accuracy, efficiency, and simplicity of the proposed scheme.

15 July 2025 04:10:33

I. INTRODUCTION

The sine-Gordon (SG) equation is a nonlinear hyperbolic partial differential equation (PDE) that plays an essential role in the modeling of many interesting problems in physical sciences, including plasma physics, solid-state physics, quantum mechanics, and nonlinear optics,

$$\frac{\partial^2 u(\mathbf{x}, t)}{\partial t^2} = \kappa^2 \Delta u(\mathbf{x}, t) + \sin u(\mathbf{x}, t), \quad \mathbf{x} \in \Omega, t > 0. \tag{1}$$

Here, $u(\mathbf{x}, t)$ is an order parameter, $\Omega \subset \mathbb{R}^d$ ($d = 1, 2, 3$) is a domain, and κ^2 is the diffusion constant.[1] The SG equation(1) has been used in nonlinear optics to describe the propagation of light pulses in optical fibers, which play the most important role in transmitting signals from communication devices, such as telephones and the internet between different locations. The SG equation has been investigated by numerous researchers, including a method for finding a new exact solution to the coupled SG equation using a modified Kudryashov approach,[5] a method for calculating a soliton solution to a generalized nonlinear Fokas–Lenells equation through an SG extension,[19] and a modified cubic B-spline differential quadrature technique for a numerical simulation of a two-dimensional SG soliton.[21] Other proposed approaches include a numerical method of a one-dimensional nonlinear SG equation by reducing the problem to a system of a first-order ordinary differential equation (ODE),[22] a meshless method based on a singular boundary method

for the numerical solutions to a nonlinear SG equation with Neumann boundary conditions,[6] and a fourth-order energy-preserving scheme for the SG equation using the Fourier pseudo-spectral method.[8] Moreover, a modified extended direct algebraic method that can handle both the SG equation and nonlinear equations in a direct and concise way,[14] a numerical method for a space–time fractional SG equation,[2] and an efficient numerical scheme for solving the two-dimensional space–time fractional SG equation within the non-rectangular domain[18] have been proposed. Several studies have also been recently conducted on the second-order accurate methods[4,20,23,24] to solve the SG equation. High-order accurate methods have also been studied.[17,26]

In this paper, we present an unconditionally stable temporally second-order accurate operator splitting scheme for a parabolic sine-Gordon equation (PSG),[3]

$$\frac{\partial u(\mathbf{x}, t)}{\partial t} = \kappa^2 \Delta u(\mathbf{x}, t) + \sin u(\mathbf{x}, t), \quad \mathbf{x} \in \Omega, t > 0. \tag{2}$$

Equation (2) can be derived from the gradient flow of the following energy functional:

$$\mathcal{E}(u) = \int_\Omega \left(\frac{\kappa^2}{2} |\nabla u|^2 + \cos u \right) d\mathbf{x}. \tag{3}$$

Phase-field modeling has attracted considerable attention in the study of two-phase systems. Mass conservation of the phase field

was considered.[9] In particular, the PSG equation provides the global well-posedness and maximum principle of the classical solution.[3]

This paper is organized as follows: In Sec. II, a numerical solution algorithm is introduced for an unconditionally stable scheme using the operator splitting method. In Sec. III, various numerical experiments are simulated to confirm the accuracy, stability, and simplicity of the proposed scheme and to show the dynamics of the PSG equation. Finally, some concluding remarks are presented in Sec. IV.

II. NUMERICAL SOLUTION ALGORITHM

Now, we present an unconditionally stable temporally second-order accurate numerical solution algorithm for the PSG equation. We use the operator splitting method to solve the PSG equation (2). For simplicity of exposition, we describe the numerical solution algorithm for the PSG equation in the two-dimensional domain $\Omega = (L_x, R_x) \times (L_y, R_y)$. Numerical solution algorithms in one- and three-dimensional spaces are described analogously. To discretize Eq. (2), let $\Omega_h = \{x_i = L_x + (i - 0.5)h, y_j = L_y + (j - 0.5)h) | 1 \le i \le N_x, 1 \le j \le N_y\}$ be the discrete computational domain, where $h = (R_x - L_x)/N_x = (R_y - L_y)/N_y$ is the uniform step size; in addition, N_x and N_y are the numbers of the grid points in the x- and y-directions, respectively. Let u_{ij}^n be the numerical approximation of $u(x_i, y_j, n\Delta t)$, where Δt is the time step. To obtain a second-order scheme, we require the following steps:[11]

$$u(\mathbf{x}, t + \Delta t) = \left(\mathcal{N}^{\Delta t/2} \circ \mathcal{L}^{\Delta t} \circ \mathcal{N}^{\Delta t/2}\right)u(\mathbf{x}, t) + \mathcal{O}\left(\Delta t^3\right), \; \mathbf{x} \in \Omega, \; t > 0,$$
(4)

where $\mathcal{N}^{\Delta t}$ and $\mathcal{L}^{\Delta t}$ are the nonlinear and linear solution operators of the PSG equation, respectively. Moreover, the operators $\mathcal{N}^{\Delta t}u(\mathbf{x}, t)$ and $\mathcal{L}^{\Delta t}u(\mathbf{x}, t)$ indicate the solutions of $u_t = \sin u$ and $u_t = \kappa^2 \Delta u$ at $t + \Delta t$, respectively. The stability and convergence of the Strang-type splitting method (4) were studied for the Allen–Cahn,[13,16,25] Cahn–Hilliard,[15] and Swift–Hohenberg[11] equations. It was theoretically proven that the second-order accuracy of the splitting method (4) is guaranteed when each operator has at least a second-order accuracy.[7] Because each operator in Eq. (4) has a temporally exact accuracy, the numerical scheme is temporally second-order accurate. The splitting method (4) can be written in three sub-steps using intermediate values as follows:

$$u^* = \mathcal{N}^{\Delta t/2}u^n,$$
(5)

$$u^{**} = \mathcal{L}^{\Delta t}u^*,$$
(6)

$$u^{n+1} = \mathcal{N}^{\Delta t/2}u^{**}.$$
(7)

Before we solve the nonlinear operator $\mathcal{N}^{\Delta t/2}$, we consider the following equation:

$$\frac{\partial v(\mathbf{x}, t)}{\partial t} = \sin(v(\mathbf{x}, t)),$$
(8)

which has a closed-form solution. If $\sin(v(\mathbf{x}, t)) = 0$, then $v(\mathbf{x}, t) = 0$. Provided that $\sin(v(\mathbf{x}, t)) \ne 0$, we can write Eq. (8) in the form

$$\frac{\partial v}{\sin v} = \partial t,$$
(9)

where we omitted the argument for simplicity of the notation. By multiplying both the denominator and the numerator on the left-hand side of Eq. (9) by $\sin v$, we have

$$\frac{\sin v}{\sin^2 v}\partial v = \partial t.$$
(10)

By using the Pythagorean trigonometric identity, we obtain

$$\frac{\sin v}{1 - \cos^2 v}\partial v = \partial t.$$
(11)

Then, by integrating both sides after using a partial fraction expansion on the left side, we have

$$\int \frac{1}{2}\left(\frac{\sin v}{1 + \cos v} + \frac{\sin v}{1 - \cos v}\right)\partial v = \int \partial t,$$
(12)

which results in

$$\frac{1}{2}\ln\frac{1 - \cos v}{1 + \cos v} = t + C(\mathbf{x}),$$
(13)

where $C(\mathbf{x}) = 0.5[\ln(1 - \cos v(\mathbf{x}, 0)) - \ln(1 + \cos v(\mathbf{x}, 0))]$. Because the cosine function is an even function, we obtain the solution to Eq. (13) as

$$v(\mathbf{x}, t) = \text{sgn}(\sin(v(\mathbf{x}, 0)))\cos^{-1}\left(\frac{1 - e^{2t+2C(\mathbf{x})}}{1 + e^{2t+2C(\mathbf{x})}}\right),$$
(14)

where $\text{sgn}(\phi)$ is the sign function, which is plus one if ϕ is positive, minus one if it is negative, and zero otherwise. Now, using the analytic solution form (14), we solve the nonlinear operator $\mathcal{N}^{\Delta t/2}$ (5) as

$$u_{ij}^* = \text{sgn}(\sin(u_{ij}^n))\cos^{-1}\left(\frac{1 - e^{\Delta t+2C_{ij}^n}}{1 + e^{\Delta t+2C_{ij}^n}}\right),$$
(15)

where $C_{ij}^n = 0.5[\ln(1 - \cos u_{ij}^n) - \ln(1 + \cos u_{ij}^n)]$.

Next, to solve the linear operator $\mathcal{L}^{\Delta t}$, we consider the diffusion equation

$$\frac{\partial v(\mathbf{x}, t)}{\partial t} = \kappa^2 \Delta v(\mathbf{x}, t).$$
(16)

We use the Fourier spectral method in (16). To solve Eq. (16) with the homogenous Neumann boundary condition, we use the discrete cosine transform. For the given data $\{v_{ij}^m | i = 1, \ldots, N_x$ and $j = 1, \ldots, N_y\}$, the discrete cosine transform is defined as follows:

$$\hat{v}_{pq}^m = \alpha_p \beta_q \sum_{i=1}^{N_x} \sum_{j=1}^{N_y} v_{ij}^m \cos(\xi_p \pi x_i) \cos(\eta_q \pi y_j).$$

The inverse discrete cosine transform is

$$v_{ij}^m = \sum_{p=1}^{N_x} \sum_{q=1}^{N_y} \alpha_p \beta_q \hat{v}_{pq}^m \cos(\xi_p \pi x_i) \cos(\eta_q \pi y_j),$$
(17)

where

$$\alpha_p = \begin{cases} \sqrt{\dfrac{1}{N_x}} & (p = 1), \\ \sqrt{\dfrac{2}{N_x}} & (p \ge 2), \end{cases} \qquad \beta_q = \begin{cases} \sqrt{\dfrac{1}{N_y}} & (q = 1) \\ \sqrt{\dfrac{2}{N_y}} & (q \ge 2), \end{cases}$$
(18)

15 July 2025 04:10:33

$\xi_p = (p-1)/L_x$, and $\eta_q = (q-1)/L_y$. Let us assume that

$$v(x, y, m\Delta t) = \sum_{p=1}^{N_x} \sum_{q=1}^{N_y} \alpha_p \beta_q \hat{v}_{pq}^m \cos(\xi_p \pi x) \cos(\eta_q \pi y). \quad (19)$$

Plugging Eq. (19) in Eq. (16) yields

$$\frac{d\hat{v}_{pq}}{dt} = -\kappa^2 \left[(\xi_p \pi)^2 + (\eta_q \pi)^2 \right] \hat{v}_{pq}. \quad (20)$$

Therefore, we obtain the following solution from Eq. (20):

$$\hat{v}_{pq}^{n+1} = \hat{v}_{pq}^n e^{-\Delta t \kappa^2 \left[(\xi_p \pi)^2 + (\eta_q \pi)^2 \right]}. \quad (21)$$

We can then solve the linear operator $\mathscr{L}^{\Delta t}$ (6) by obtaining the numerical solution u_{ij}^{**} using Eqs. (17) and (21), i.e.,

$$\hat{u}_{pq}^{**} = \hat{u}_{pq}^* e^{-\Delta t \kappa^2 \left[(\xi_p \pi)^2 + (\eta_q \pi)^2 \right]} \quad (22)$$

and

$$u_{ij}^{**} = \sum_{p=1}^{N_x} \sum_{q=1}^{N_y} \alpha_p \beta_q \hat{u}_{pq}^{**} \cos(\xi_p \pi x_i) \cos(\eta_q \pi y_j). \quad (23)$$

The final sub-step (7) can also be solved analogously as (15),

$$u_{ij}^{n+1} = \text{sgn}(\sin(u_{ij}^{**})) \cos^{-1} \left(\frac{1 - e^{\Delta t + 2C_{ij}^{**}}}{1 + e^{\Delta t + 2C_{ij}^{**}}} \right), \quad (24)$$

where $C_{ij}^{**} = 0.5[\ln(1 - \cos u_{ij}^{**}) - \ln(1 + \cos u_{ij}^{**})]$. More details regarding the procedure and the definitions of the notions are provided in Ref. 12. We note that the proposed numerical algorithm is an unconditionally stable scheme. First, we suppose that the nth solution satisfies $|u_{ij}^n| \leq \pi$. In the first sub-step (5), the solution u^* is bounded by π from Eq. (15) for any time step Δt, i.e.,

$$|u_{ij}^*| \leq \pi. \quad (25)$$

The stability condition of a semi-analytical Fourier spectral method for the Allen–Cahn equation was presented in Ref. 12. In the second sub-step (6), substituting Eq. (22) in Eq. (23),

$$u_{ij}^{**} = \sum_{p=1}^{N_x} \sum_{q=1}^{N_y} \alpha_p \beta_q \hat{u}_{pq}^* e^{-\Delta t \kappa^2 \left[(\xi_p \pi)^2 + (\eta_q \pi)^2 \right]} \times \cos(\xi_p \pi x_i) \cos(\eta_q \pi y_j). \quad (26)$$

The u_{ij}^{**} in Eq. (26) is a solution of the heat equation for an initial condition u_{ij}^*. Because it is well known that the heat equation with homogeneous Neumann boundary condition satisfies the maximum principle, we have

$$\max_{ij} |u_{ij}^{**}| \leq \max_{ij} |u_{ij}^*| \leq \pi. \quad (27)$$

Finally, in the last sub-step (7), the following inequality is established because $|u_{ij}^{**}|$ is bounded by π from Eq. (15) for any time step Δt,

$$|u^{n+1}| \leq \pi. \quad (28)$$

Therefore, the proposed method is unconditionally stable regardless of the time step Δt and the maximum norm of each solution is bounded by π, which implies the boundedness of the numerical solutions.

III. NUMERICAL EXPERIMENTS

We use the second-order operator splitting scheme (6) to solve the PSG equation. Unless otherwise mentioned, we use numerical parameters as $N_x = 128$, $N_y = 128$, and $N_z = 128$ for grid points of the spatial discretization, $\kappa = 0.2$ and $\Omega = (-\pi, \pi)^d$, where $d = 1, 2, 3$. Each nonlinear and linear operator is solved using (15) and (23), respectively.

A. Convergence and stability

We investigate the convergence and stability of the proposed scheme with respect to the time step. For the test, we take $\phi(x, 0) = \cos(x)$ as the initial condition. First, we evaluate the errors and compare with the reference solution and convergence rate. Let $\log_2(\|\mathbf{e}_{N_x}^{N_t}\| / \|\mathbf{e}_{N_x}^{2N_t}\|)$ be the temporal convergence rate. Table I lists the errors with a reference solution and temporal convergence rates for the proposed method in the one-dimensional space with various values of Δt and a fixed space step size $h = 2\pi/N_x$ at $t = 1$. According to Table I, we confirm that this scheme guarantees a second-order convergence with respect to time step. Figure 1 shows the evolution of the energy functional (3) with reference energy $\mathscr{E}_{ref}$ (solid line) and different time steps $\Delta t = 1$ (circle), 2^{-2} (triangle), and 2^{-4} (dot). The energy monotonically decreases with time, and the numerical energies fit well with the reference energy for all values of Δt. In Fig. 2, to check the stability condition, we use random perturbations between -0.1 and 0.1 as the initial condition in each case. Figures 2(a) and 2(b) show the dynamics of the 1D PSG equation with $\Delta t = 0.1$ and $\Delta t = 10$, respectively. In Fig. 2(b), the solution does not blow up and shows similar dynamics as the solution illustrated in Fig. 2(a), which uses a relatively small time step compared to Fig. 2(b). From the stable results using a time step 100 times larger than 0.1, we can confirm the unconditional stability of the proposed scheme.

B. Boundedness of the numerical solutions

To ensure that the PSG equation satisfies the boundedness of the numerical solutions, we consider the random perturbation between -1 and 1 as an initial condition with $N_x = 2^8$ within the 1D

TABLE I. l_2-norm errors and convergence rates for the proposed method with fixed h and various Δt. Here, $h = 2\pi/2^{10}$, $\Delta t = 2^{-4}$, and $\Delta t_{ref} = 2^{-15}$ are used with $t = 1$.

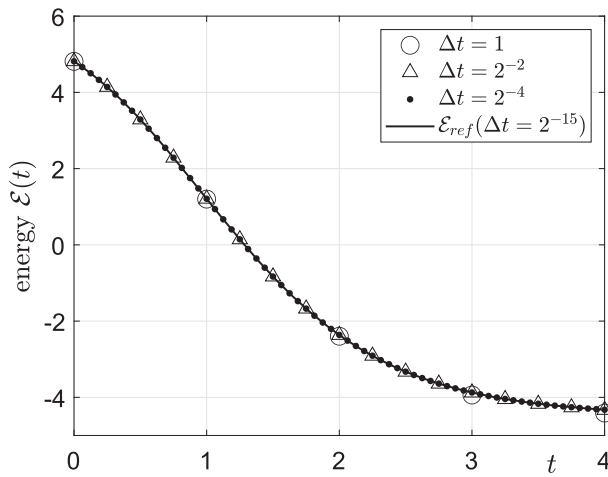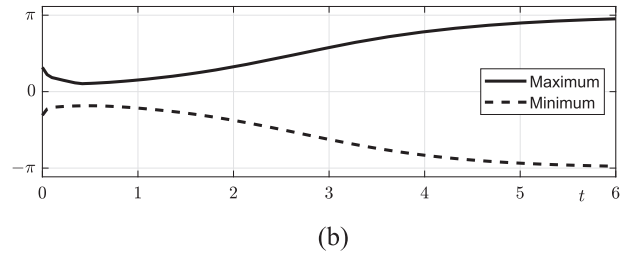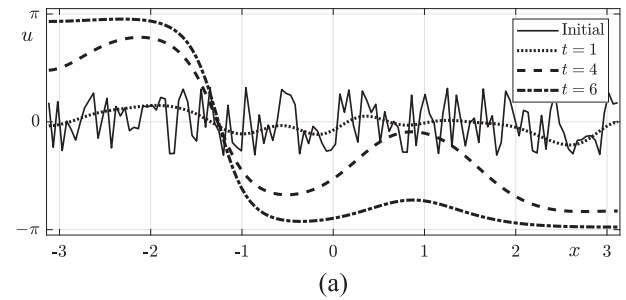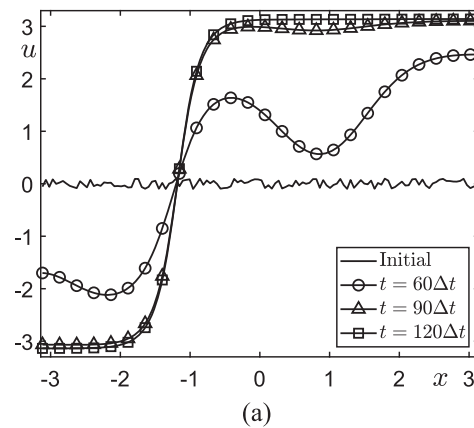| Case	Δt	Rate	$\Delta t/2$	Rate	$\Delta t/4$	Rate	$\Delta t/8$
l_2-error	$1.036\,88 \times 10^{-5}$	1.9997	$2.592\,80 \times 10^{-6}$	1.9999	$6.482\,35 \times 10^{-7}$	2.0000	$1.620\,57 \times 10^{-7}$

FIG. 1. Energy evolution with different time steps.

FIG. 3. (a) Temporal dynamics of the one-dimensional PSG equation with random perturbation between −1 and 1 and (b) maximum and minimum values of the solution with $N_x = 2^8$ and $\Delta t = 0.05$.

domain $\Omega \in (-\pi, \pi)$. Here, $\Delta t = 0.05$ is used. Figure 3(a) shows the temporal dynamics of the 1D PSG equation with a randomly perturbed initial condition. Figure 3(b) shows the maximum and minimum values of the solution over time $t = 0$ to $t = 10$. In Figs. 3(a) and 3(b), we can see that the values of the solution are bounded by π. This shows that the PSG equation satisfies the boundedness of the numerical solutions.

C. Linear stability analysis

We consider a linear stability analysis of the PSG equation. At $u(\mathbf{x}, t) = 0$, the nonlinear term $\sin u(\mathbf{x}, t)$ can be linearized using the Taylor expansion as $\sin u(\mathbf{x}, t) \approx u(\mathbf{x}, t)$. Therefore, the linearized PSG equation is as follows:

$$\frac{\partial u(\mathbf{x}, t)}{\partial t} = \kappa^2 \Delta u(\mathbf{x}, t) + u(\mathbf{x}, t). \tag{29}$$
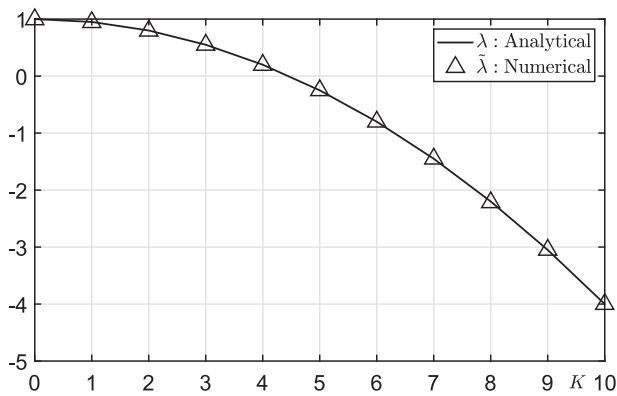
For the positive integers K_i and $\mathbf{x} \in \mathbb{R}^d$ where $d = 1, 2, 3$ is the space dimension, we can obtain

$$u(\mathbf{x}, t) = \alpha(t) \prod_{i=1}^{d} \cos(K_i x_i), \tag{30}$$

where $\alpha(t)$ is the amplitude of $u(\mathbf{x}, t)$. If $d = 3$, then $\mathbf{x} = (x_1, x_2, x_3)$. Substituting $u(\mathbf{x}, t)$ in Eq. (30) into Eq. (29), we have

$$\alpha'(t) \prod_{i=1}^{d} \cos(K_i x_i) = -\kappa^2 \alpha(t) \sum_{j=1}^{d} K_j^2 \prod_{i=1}^{d} \cos(K_i x_i)$$

$$+ \alpha(t) \prod_{i=1}^{d} \cos(K_i x_i). \tag{31}$$

FIG. 2. Temporal dynamics of the one-dimensional PSG equation with random perturbations between −0.1 and 0.1 for the initial condition, with different time steps (a) $\Delta t = 0.1$ and (b) $\Delta t = 10$.

FIG. 4. Analytical and numerical growth rates of the PSG equation for different mode numbers K with $\kappa = \sqrt{0.05}$, $\alpha(0) = 0.1$, $\Delta t = h^2$, and $T = 500\Delta t$.

By dividing $\prod_{i=1}^{d} \cos(K_i x_i)$ on the both sides of Eq. (31), we obtain

$$\alpha'(t) = \left(1 - \kappa^2 \sum_{j=1}^{d} K_j^2\right)\alpha(t). \tag{32}$$

We can analytically solve the ordinary differential equation (32) and find the solution as follows: $\alpha(t) = \alpha(0)e^{\lambda t}$, where $\lambda = 1 - \kappa^2 \sum_{j=1}^{d} K_j^2$ is the analytic growth rate. We then define the numerical growth rate

as

$$\tilde{\lambda} = \frac{1}{T} \log \frac{\|u^{N_t}\|_{\infty}}{\alpha(0)}. \tag{33}$$

In a one-dimensional space $\Omega = (-\pi, \pi)$, we test the linear stability experiments with the initial condition $u(x, 0) = 0.1 \cos(Kx)$, where $K = 0, 1, \ldots, 10$. As shown in Fig. 4, numerical growth rates $\tilde{\lambda}$ approximate well the analytic growth rates λ for each K. As mode K increases, the growth rate decreases. In particular, the growth rates have positive values only when K is less than or equal to 4.
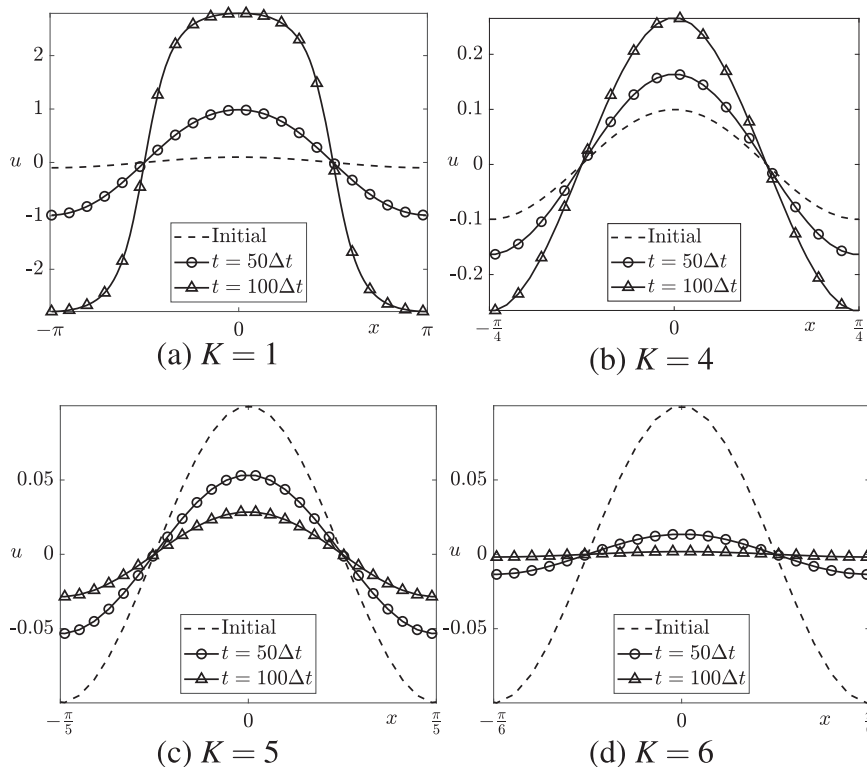
In Fig. 5, we simulate the 1D PSG equation to check how the numerical solutions grow depending on the mode number K. Only one-period solutions are shown. As it can be seen from the results in Figs. 4 and 5, the growth rate of the solution decreases as K increases. In particular, when mode K is greater than 4, the growth rates become negative, and the solutions are damped.

D. Growth simulation
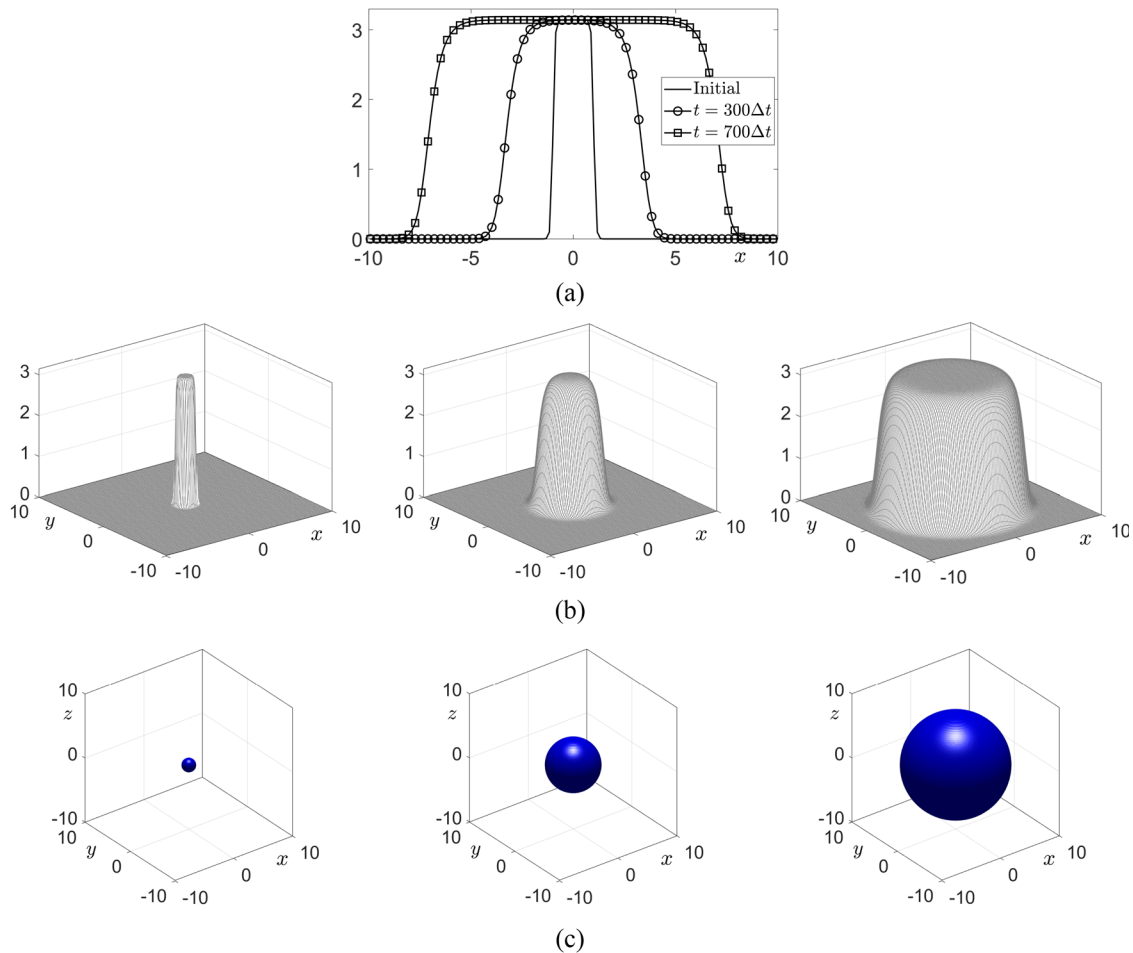
Let us consider the following initial condition:

$$u(\mathbf{x}, 0) = \frac{\pi}{2}\left(1 + \tanh\left(\frac{1 - |\mathbf{x}|}{0.1}\right)\right), \quad \mathbf{x} \in (-10, 10)^d \ (d = 1, 2, 3), \tag{34}$$

which implies that the initial values are between 0 and π. In this simulation, we consider the numerical parameters as $\Delta t = 0.025$, $N_x = 128$, $N_y = 128$, and $N_z = 128$. Figures 6(a)–6(c) show the snapshots of the evolution of solutions of the PSG equation with the initial condition (34) in one-, two-, and three-dimensional spaces, respectively.

(a) $K = 1$

(b) $K = 4$

(c) $K = 5$

(d) $K = 6$

FIG. 5. Snapshots of the evolution of the solutions for the one-dimensional PSG equation with the initial condition $u(x, 0) = 0.1 \cos(Kx)$. The values of K are shown in each figure (a) $K = 1$, (b) $K = 4$, (c) $K = 5$, and (d) $K = 6$.

(a)

(b)

(c)

FIG. 6. (a)–(c) are snapshots of the evolution of the solutions of the PSG equation with the initial condition (34) for 1D, 2D, and 3D spaces, respectively. Here, the isosurface plots are at a level of $u = 0.1$.

IV. CONCLUSIONS

Little research has been conducted on the specificity and dynamics of the parabolic sine-Gordon (PSG) equation. The main novelty of this study is to develop a fast and accurate numerical method for the PSG equation. We presented an unconditionally stable second-order accurate numerical method for the PSG equation. We solved linear and nonlinear equations using a Fourier spectral method and a closed-form solution. Because each split operator has a temporally exact accuracy, it can be extended to a high-order accurate method. To demonstrate the superior performance of the proposed scheme, we performed several computational experiments. We showed the second-order accuracy and unconditionally stability of the proposed scheme. The growth rate was analyzed using linear stability analysis, and it was confirmed that it was in good agreement with the simulation results. Through the computational tests, we confirmed the accuracy, efficiency, and simplicity of the proposed scheme. In future work, the proposed second-order operator splitting scheme will be extended to

numerically solve the spatial fractional-order parabolic-type sine-Gordon equation.[10,27]

AUTHOR DECLARATIONS

Conflict of Interest

The authors have no conflicts of interest to disclose.

DATA AVAILABILITY

The data that support the findings of this study are available from the corresponding author upon reasonable request.

REFERENCES

[1] K. K. Ali, M. S. Osman, and M. Abdel-Aty, "New optical solitary wave solutions of Fokas–Lenells equation in optical fiber via sine-Gordon expansion method," Alexandria Eng. J. **59**(3), 1191–1196 (2020).

[2] M. Ahmadinia and Z. Safari, "Analysis of local discontinuous Galerkin method for time-space fractional sine-Gordon equations," Appl. Numer. Math. **148**, 1–17 (2020).

[3] X. Cheng, D. Li, C. Quan, and W. Yang, "On a parabolic sine-Gordon model," Numer. Math. Theory Methods Appl. **14**(4), 1068–1084 (2021).

[4] Y. Fu, W. Cai, and Y. Wang, "A linearly implicit structure-preserving scheme for the fractional sine-Gordon equation based on the IEQ approach," Appl. Numer. Math. **160**, 368–385 (2021).

[5] K. Hosseini, P. Mayeli, and D. Kumar, "New exact solutions of the coupled sine-Gordon equations in nonlinear optics using the modified Kudryashov method," J. Mod. Opt. **65**(3), 361–364 (2018).

[6] Y. Ji, "Meshless singular boundary method for nonlinear sine-Gordon equation," Math. Probl. Eng. **2018**, 6460480.

[7] T. Jahnke and C. Lubich, "Error bounds for exponential operator splittings," BIT Numer. Math. **40**(4), 735–744 (2000).

[8] C. Jiang, J. Sun, H. Li, and Y. Wang, "A fourth-order AVF method for the numerical integration of sine-Gordon equation," Appl. Math. Comput. **313**, 144–158 (2017).

[9] M. Kwakkel, M. Fernandino, and C. A. Dorao, "A redefined energy functional to prevent mass loss in phase-field methods," AIP Adv. **10**(6), 065124 (2020).

[10] H. G. Lee, "A second-order operator splitting Fourier spectral method for fractional-in-space reaction-diffusion equations," J. Comput. Appl. Math. **333**, 395–403 (2018).

[11] H. G. Lee, "A semi-analytical Fourier spectral method for the Swift–Hohenberg equation," Comput. Math. Appl. **74**(8), 1885–1896 (2017).

[12] H. G. Lee and J.-Y. Lee, "A semi-analytical Fourier spectral method for the Allen–Cahn equation," Comput. Math. Appl. **68**(3), 174–184 (2014).

[13] H. G. Lee and J. Y. Lee, "A second order operator splitting method for Allen–Cahn type equations with nonlinear source terms," Physica A **432**, 24–34 (2015).

[14] D. Lu, A. R. Seadawy, and M. Arshad, "Elliptic function solutions and travelling wave solutions of nonlinear Dodd–Bullough–Mikhailov, two-dimensional Sine-Gordon and coupled Schrödinger–KdV dynamical models," Results Phys. **10**, 995–1005 (2018).

[15] D. Li and C. Quan, "On the energy stability of Strang-splitting for Cahn–Hilliard," arXiv:2107.05349 (2021).

[16] D. Li, C. Quan, and T. Tang, "Energy dissipation of Strang splitting for Allen–Cahn," arXiv:2108.05214 (2021).

[17] F. Martin-Vergara, F. Rus, and F. R. Villatoro, "Padé schemes with Richardson extrapolation for the sine-Gordon equation," Commun. Nonlinear Sci. Numer. Simul. **85**, 105243 (2020).

[18] F. Mirzaee, S. Rezaei, and N. Samadyar, "Numerical solution of two-dimensional stochastic time-fractional Sine–Gordon equation on non-rectangular domains using finite difference and meshfree methods," Eng. Anal. Boundary Elem. **127**, 53–63 (2021).

[19] A. K. Mittal, "A stable time-space Jacobi pseudospectral method for two-dimensional sine-Gordon equation," J. Appl. Math. Comput. **63**, 239–264 (2020).

[20] A. H. Msmali, M. Tamsir, and A. A. H. Ahmadini, "Crank–Nicolson-DQM based on cubic exponential B-splines for the approximation of nonlinear Sine-Gordon equation," Ain Shams Eng. J. **12**, 4091–4097 (2021).

[21] H. S. Shukla, M. Tamsir, and V. K. Srivastava, "Numerical simulation of two dimensional sine-Gordon solitons using modified cubic B-spline differential quadrature method," AIP Adv. **5**(1), 017121 (2015).

[22] H. S. Shukla and M. Tamsir, "Numerical solution of nonlinear sine–Gordon equation by using the modified cubic B-spline differential quadrature method," Beni-Seuf Univ. J. Basic Appl. Sci. **7**(4), 359–366 (2018).

[23] F. Ureña, L. Gavete, A. García, J. J. Benito, and A. M. Vargas, "Solving second order non-linear hyperbolic PDEs using generalized finite difference method (GFDM)," J. Comput. Appl. Math. **363**, 1–21 (2020).

[24] J.-Y. Wang and Q.-A. Huang, "A family of effective structure-preserving schemes with second-order accuracy for the undamped sine–Gordon equation," Comput. Math. Appl. **90**, 38–45 (2021).

[25] X. Yang, "Error analysis of stabilized semi-implicit method of Allen–Cahn equation," Discrete Contin. Dyn. Syst. B **11**(4), 1057 (2009).

[26] Z. Xing, L. Wen, and W. Wang, "An explicit fourth-order energy-preserving difference scheme for the Riesz space-fractional Sine-Gordon equations," Math. Comput. Simul. **181**, 624–641 (2021).

[27] Y. Zhou and Z. Luo, "An optimized Crank–Nicolson finite difference extrapolating model for the fractional-order parabolic-type sine-Gordon equation," Adv. Differ. Equations **2019**, 1.